Electronic Supplementary Material (ESI) for Energy Advances.

Supporting Information

Universal synthesis strategy for preparation of transition metal oxide electrocatalysts doped with noble metal single atoms for oxygen evolution reaction

Jingyao Wang, Yiming Zhu, Xuepeng Zhong, Zhiwei Hu, Wei-Hsiang Huang, Chih-Wen Pao, Hongfei Cheng, Nicolas Alonso-Vante*, and Jiwei Ma**

Figures:

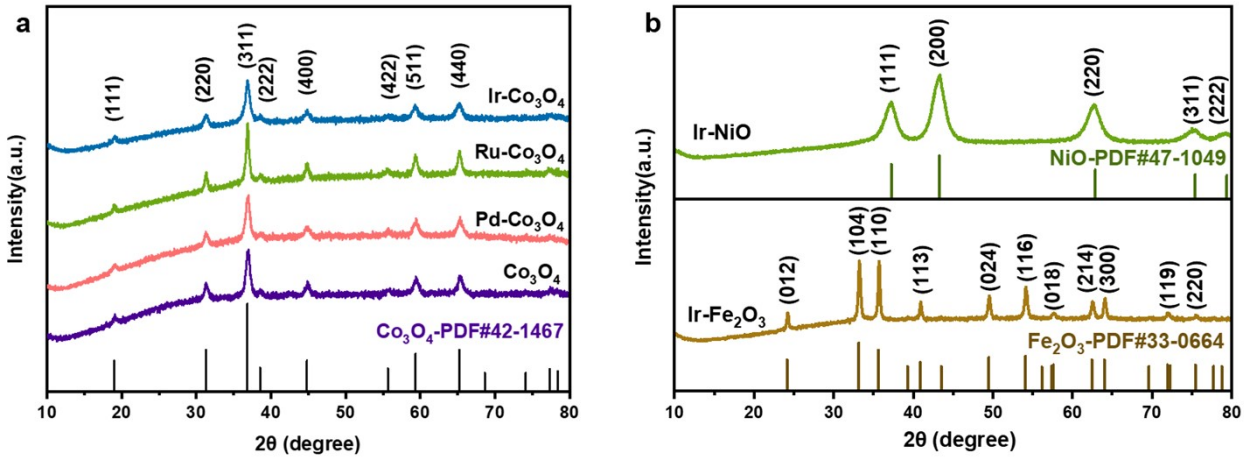

Figure S1. X-ray diffraction (XRD) patterns of (a) Ir-Co_3O_4, Ru-Co_3O_4, Pd-Co_3O_4, and Co_3O_4. (b) Ir-NiO, and Ir-Fe_2O_3.

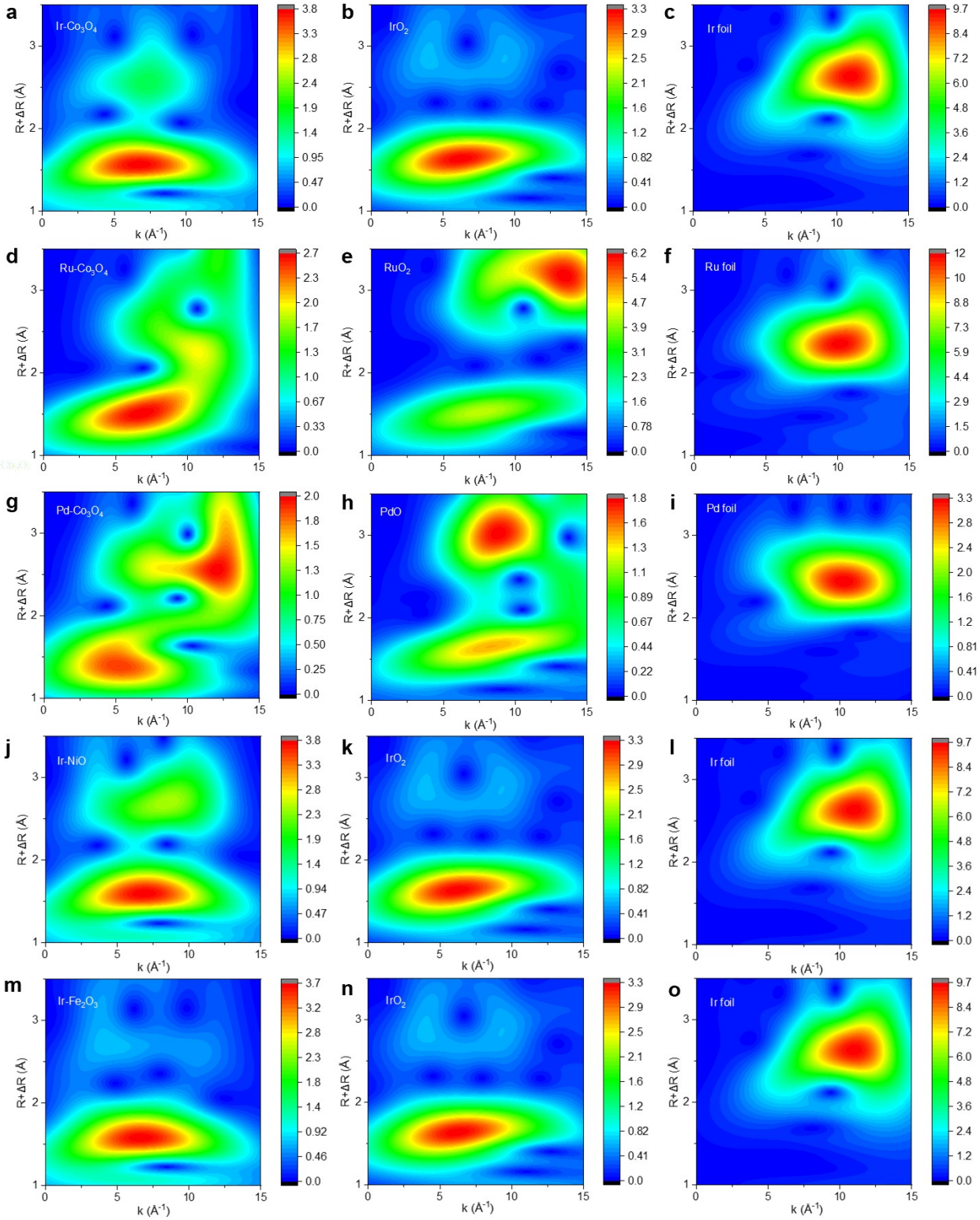

Figure S2. The wavelet transforms for the k^3-weighted EXAFS signals of (a-c) Ir-Co_3O_4, IrO_2, and Ir foil. (d-f) Ru-Co_3O_4, RuO_2, and Ru foil. (g-i) Pd-Co_3O_4, PdO, and Pd foil. (j-l) Ir-NiO, IrO_2, and Ir foil. (m-o) Ir-Fe_2O_3, IrO_2, and Ir foil.

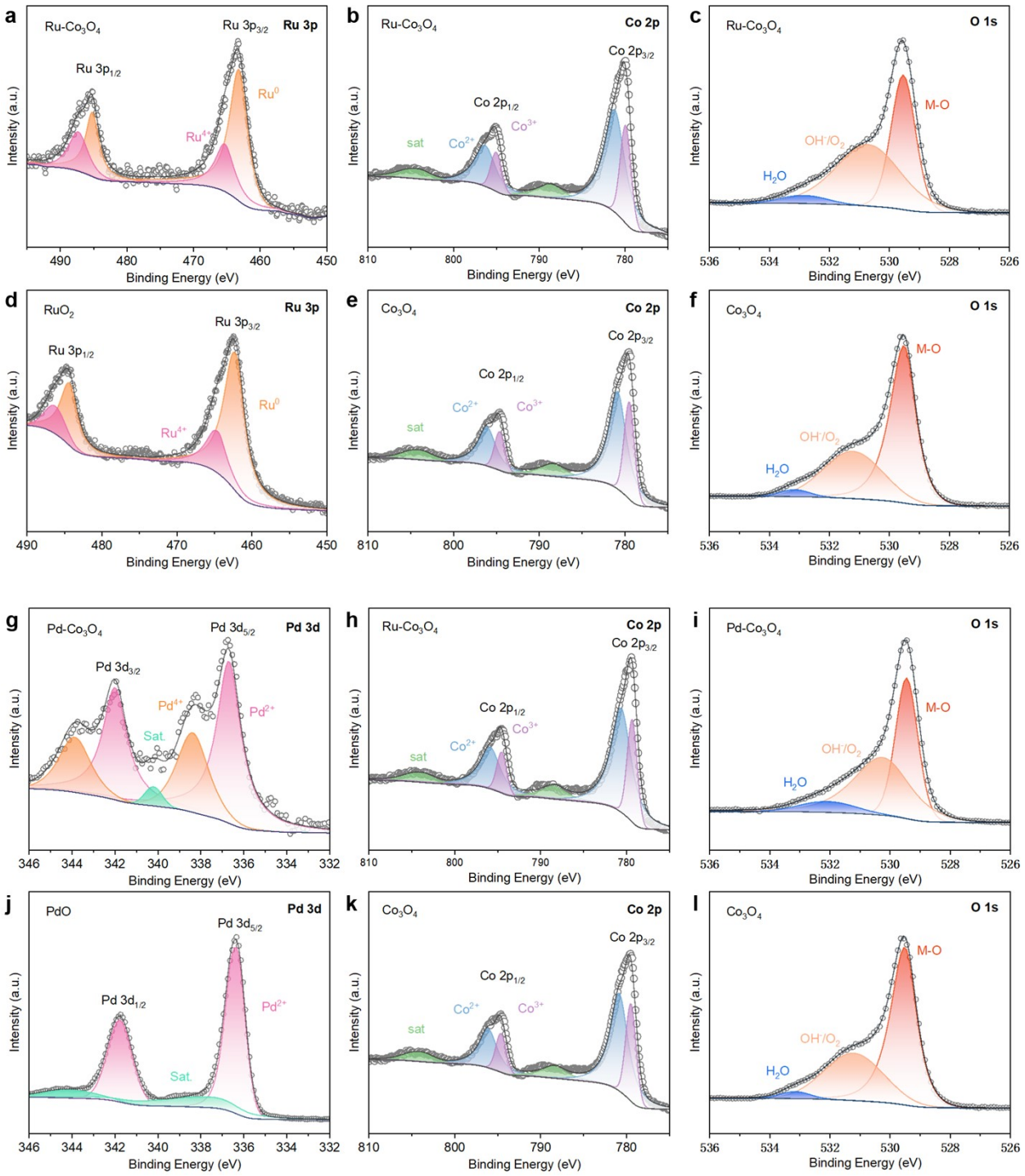
a
Ru-Co3O4
Ru 3p
Ru 3p3/2
Ru 3p1/2
Ru0
Ru4+
Intensity (a.u.)
Binding Energy (eV)
b
Ru-Co3O4
Co 2p
Co 2p3/2
Co 2p1/2
Co3+
sat
Co2+
c
Ru-Co3O4
O 1s
M-O
OH-/O2
H2O
d
RuO2
Ru 3p
e
Co3O4
Co 2p
f
Co3O4
O 1s
g
Pd-Co3O4
Pd 3d
Pd 3d5/2
Pd 3d3/2
Pd4+
Pd2+
Sat.
h
Ru-Co3O4
Co 2p
i
Pd-Co3O4
O 1s
j
PdO
Pd 3d
Pd 3d5/2
Pd 3d1/2
Pd2+
Sat.
k
Co3O4
Co 2p
l
Co3O4
O 1s

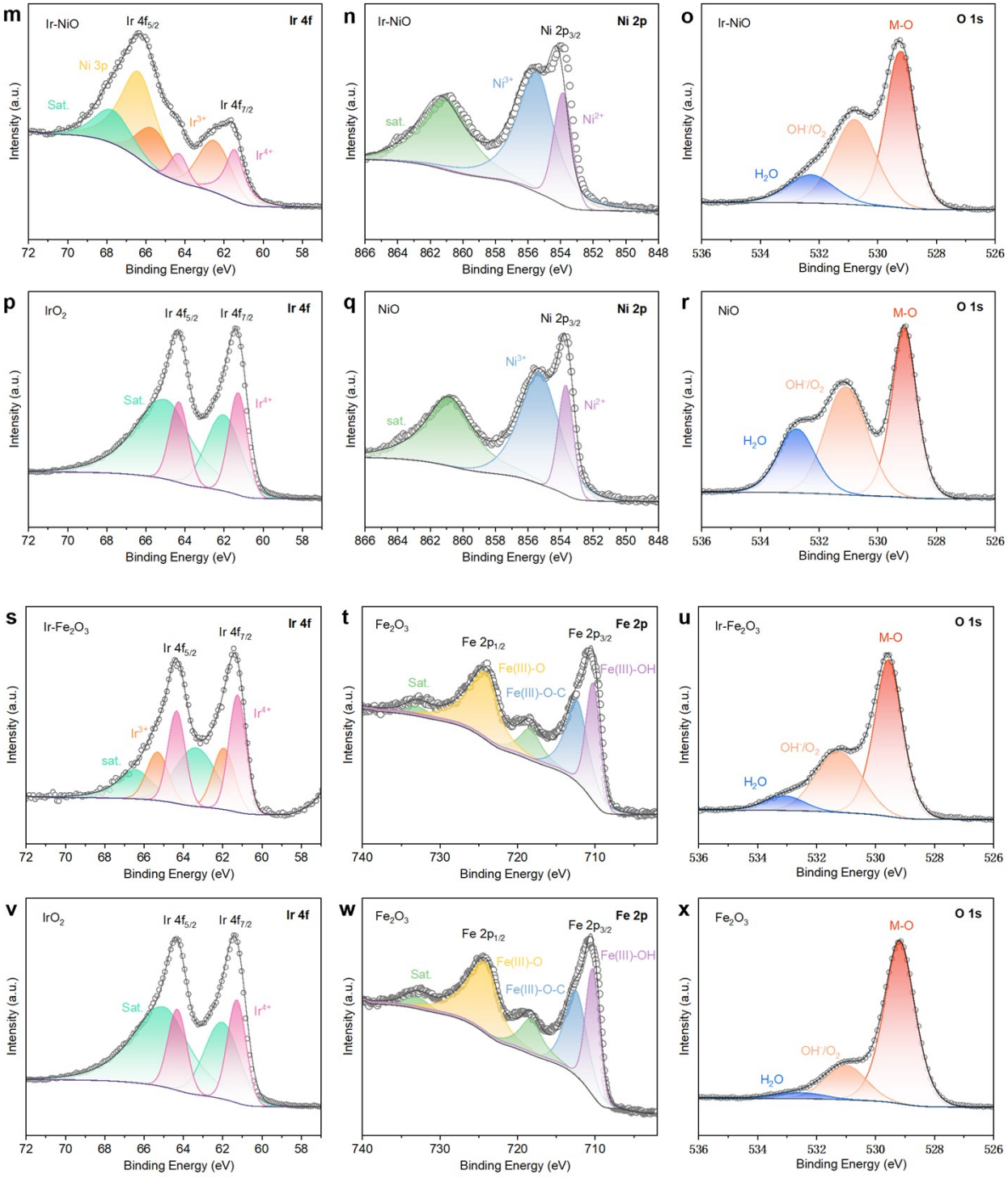

Figure S3. Photoemission lines: (a, d) Ru 3*p* of Ru-Co_3O_4 and RuO_2. (b, e) Co 2*p* and (c,f) O 1*s* of Ru-Co_3O_4 and Co_3O_4. (g, j) Pd 3*d* of Pd-Co_3O_4, and PdO. (h, k) Co 2*p*, and (i, l) O 1*s* of Pd-Co_3O_4 and Co_3O_4. (m, p) Ir 4*f* of Ir-NiO, and IrO_2. (n, q) Ni 2*p*, and (o, r) O 1*s* of Ir-NiO, and NiO. (s, v) Ir 4*f* of Ir-Fe_2O_3, and IrO_2. (t, w) Fe 2*p*, and (u, x) O 1*s* of Ir-Fe_2O_3, and Fe_2O_3.

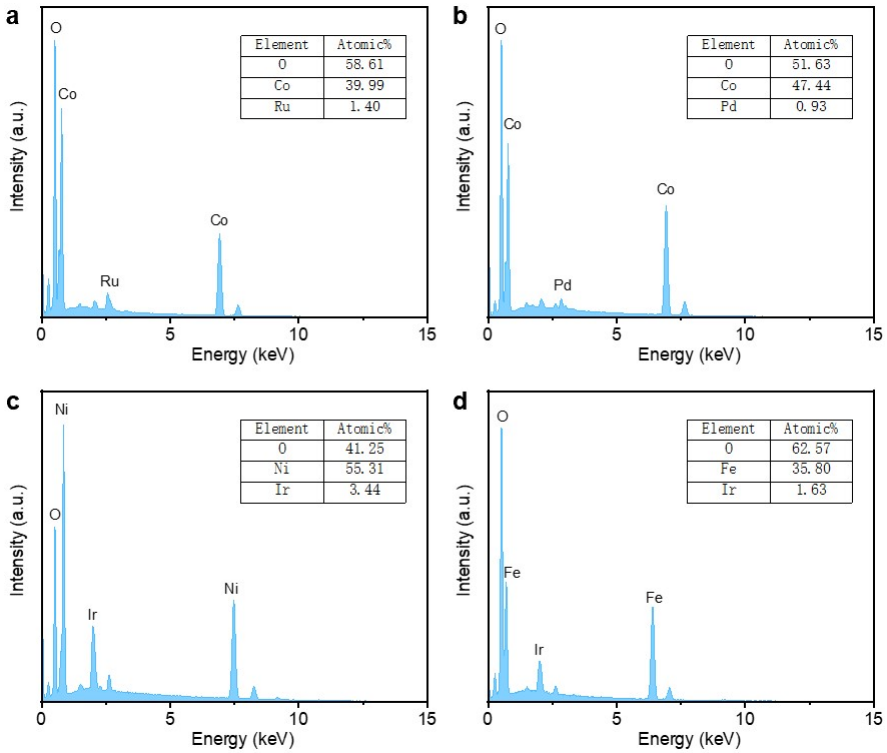

Figure S4. SEM-EDS spectra of (a) Ru-Co_3O_4, (b) Pd-Co_3O_4, (c) Ir-NiO, and (d) Ir-Fe_2O_3.

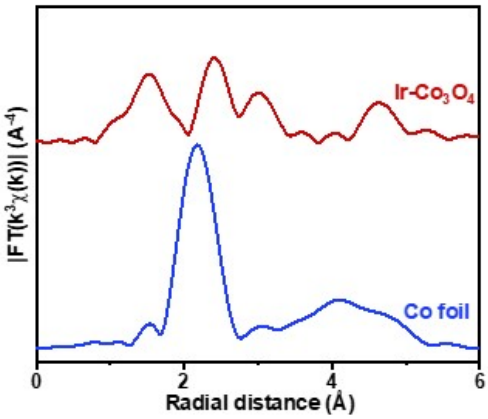

Figure S5. Co-*K* edge EXAFS spectra of Ir-Co_3O_4 and Co foil.

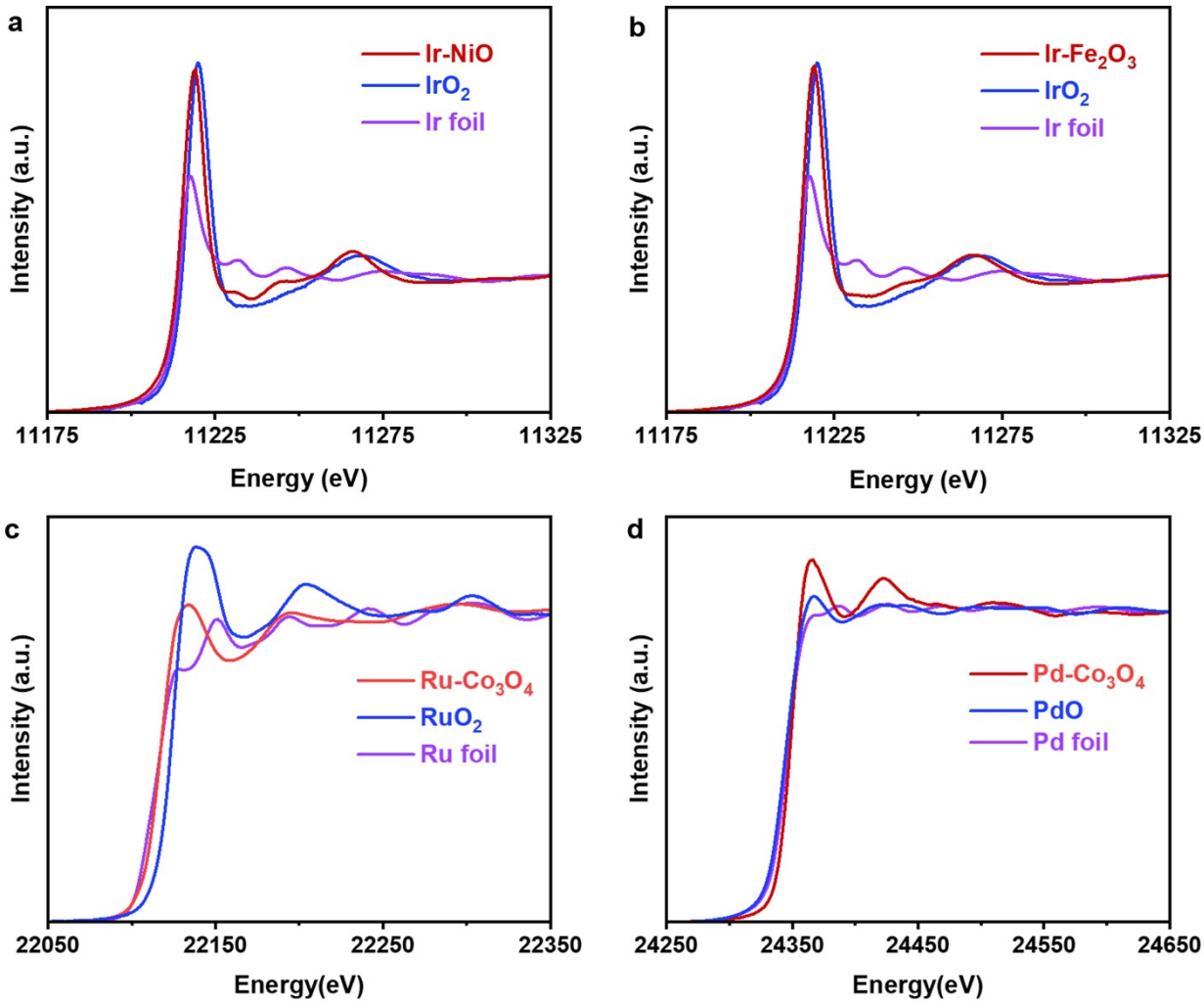

Figure S6. The normalized Ir-L_3 edge XANES spectra of (a) Ir-NiO, Ir foil, and IrO_2. (b) Ir-Fe_2O_3, Ir foil, and IrO_2. (c) The normalized Ru-*K* edge XANES spectra of Ru- Co_3O_4, Ru foil, and RuO_2. (d) The normalized Pd-*K* edge XANES spectra of Pd-Co_3O_4, Pd foil, and PdO.

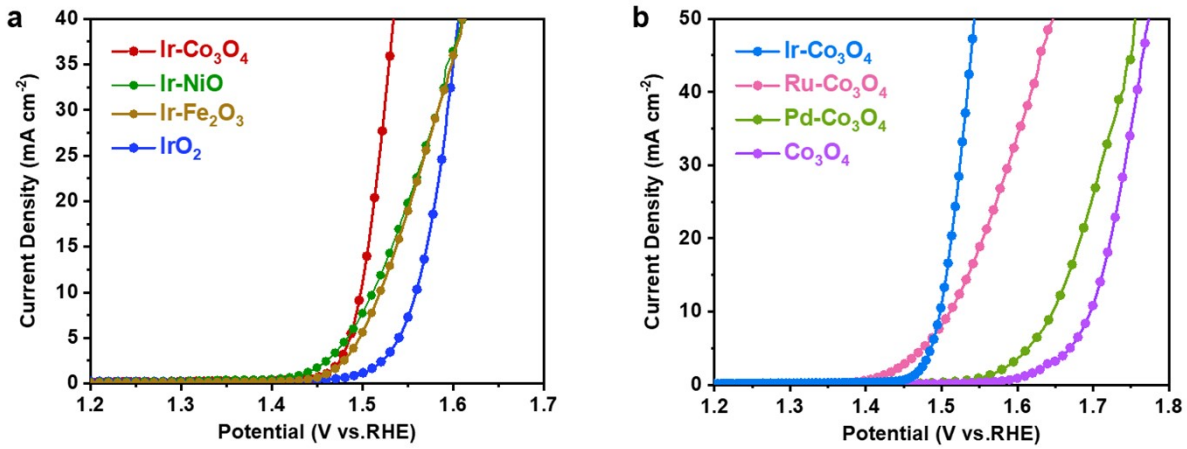

Figure S7. LSV curves of (a) Ir-Co_3O_4, Ir-NiO, Ir-Fe_2O_3, and IrO_2, (b) Ir-Co_3O_4, Ru-Co_3O_4, Pd-Co_3O_4, and Co_3O_4 collected at a scanning rate of 5 mV s^{-1} in 0.5 M H_2SO_4 solution.

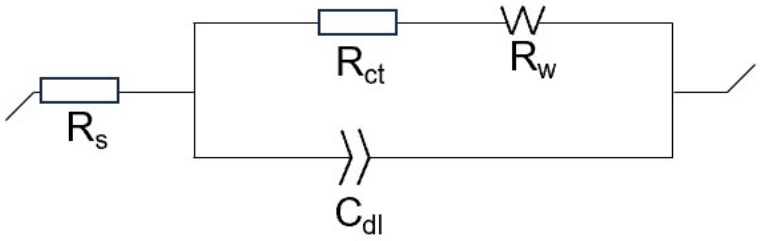

Figure S8. The equivalent circuit section applied in the EIS testing of the catalysts. Electrolyte, Charge transfer, and Warburg resistance are R_s, R_{ct}, and R_w, respectively. The double layer capacitance is C_{dl}.

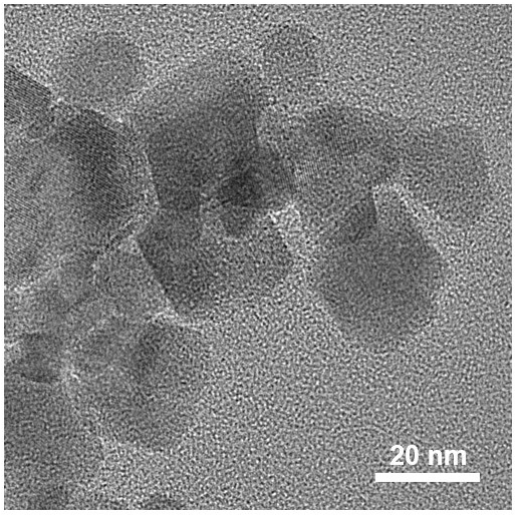

Figure S9. TEM image of Co_3O_4.

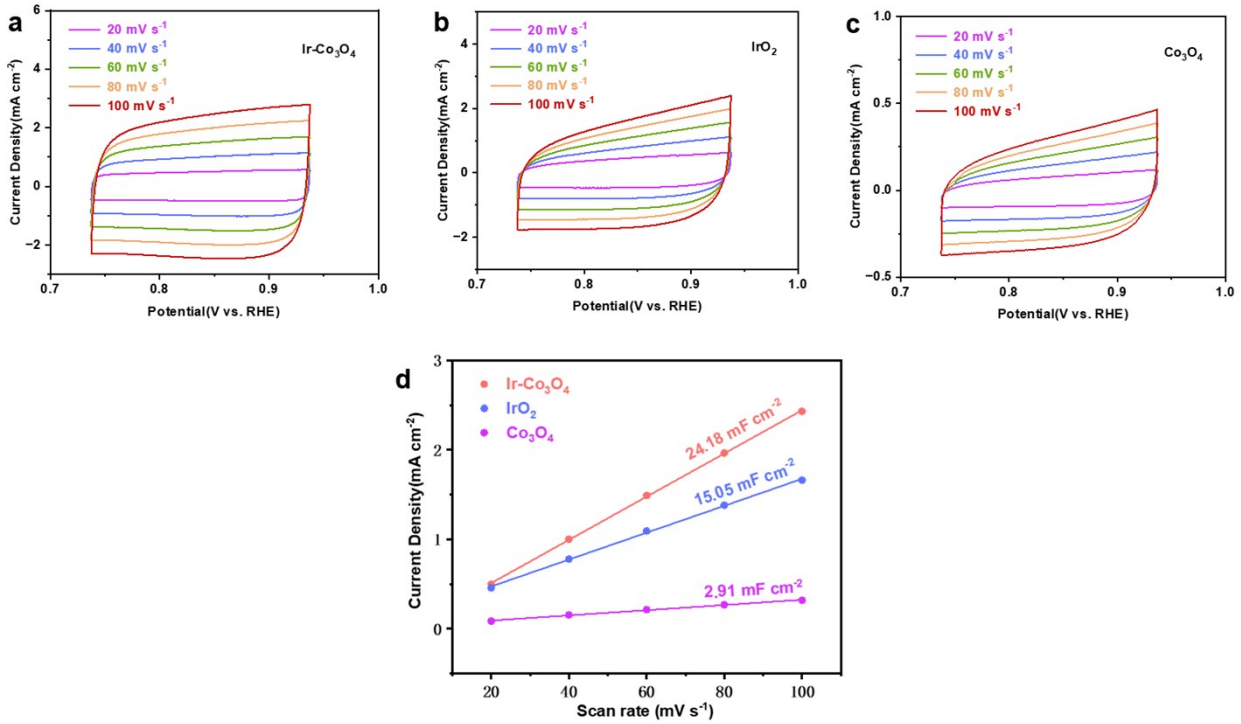

Figure S10. Electrochemical cyclic voltammetry scans were recorded for (a) Ir-Co_3O_4, (b) IrO_2, and (c) Co_3O_4. Scan rates are 20, 40, 60, 80 and 100 mV s^{-1}. (d) Linear fitting of the capacitive currents versus cyclic voltammetry scan rates for these catalysts.

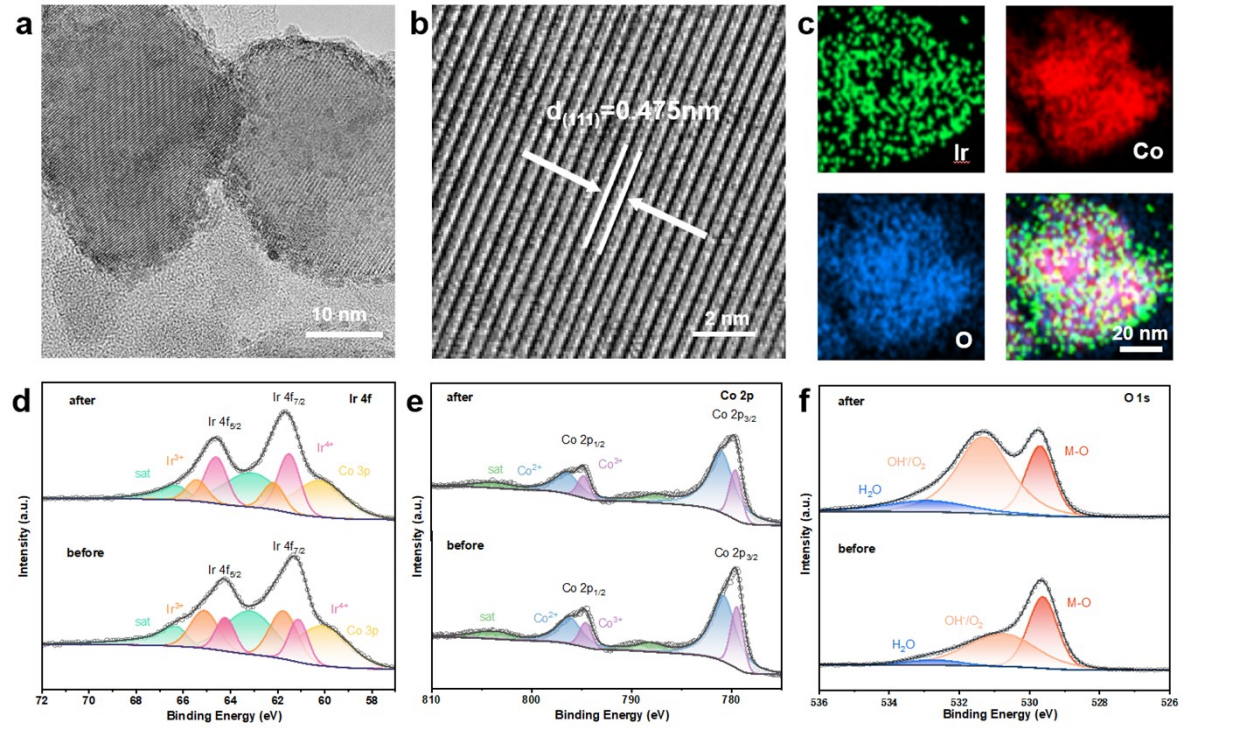

Figure S11. (a) TEM image, (b) HR-TEM image, (c) EDS elemental mappings of Ir-Co_3O_4 after stability test. (d) Ir 4*f*, (e) Co 2*p*, (f) O1*s* XPS spectrum of Ir-Co_3O_4 before and after stability test.

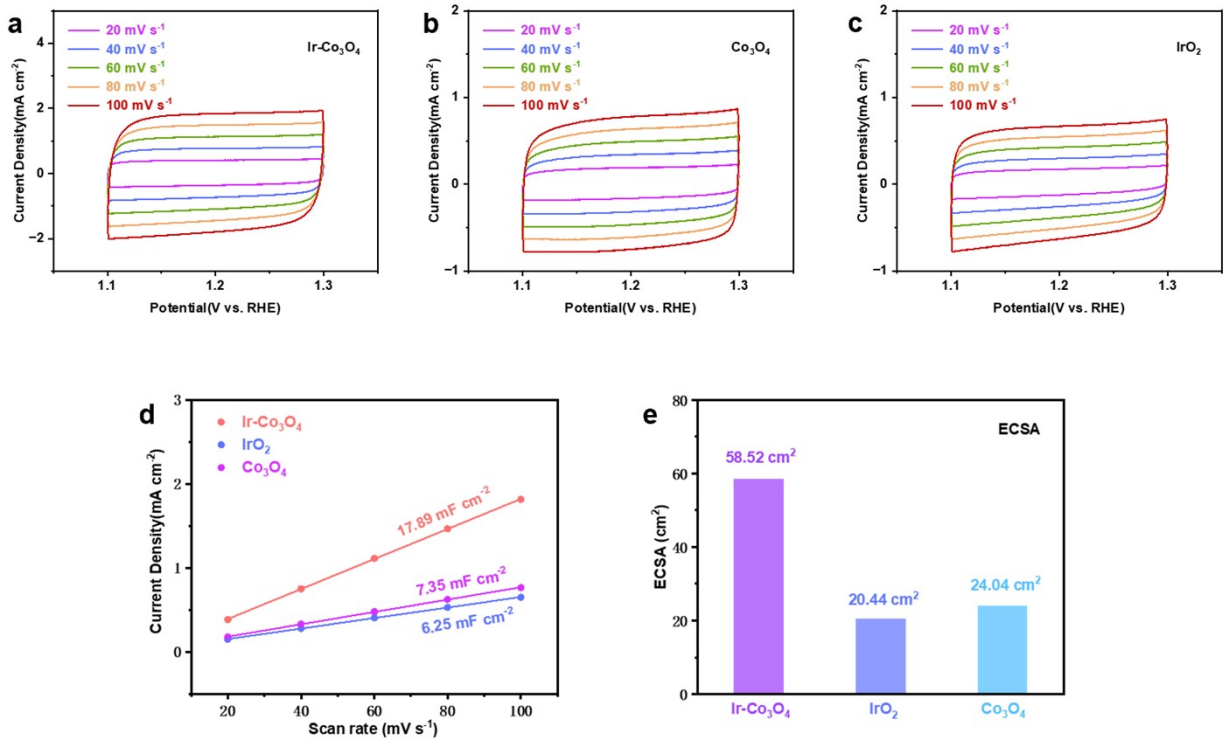

Figure S12. Electrochemical cyclic voltammetry scans were recorded for (a) Ir-Co_3O_4, (b) Co_3O_4, and (c) IrO_2. Scan rates are 20, 40, 60, 80, and 100 mV s^{-1}. (d) Linear fitting of the capacitive currents versus cyclic voltammetry scan rates for these catalysts. (e) The calculated ECSA values for Ir-Co_3O_4, IrO_2, and Co_3O_4 in 1.0 M KOH.

Tables:

Table S1. Fit goodness and R-factor of XRD refinements for Ir-Co_3O_4 and Co_3O_4.

Compounds	R_F	R_B	R_P	R_{WP}	χ^2
Ir-Co_3O_4	0.309%	0.314%	0.286%	0.462%	3.46
Co_3O_4	0.816%	0.598%	0.228%	0.293%	1.64

Table S2. Results of XRD refinements for Ir-Co_3O_4 and Co_3O_4.

Compounds	*a* (Å)	*b* (Å)	*c* (Å)	*V* (Å^3)
Ir-Co_3O_4	8.102	8.102	8.102	531.9
Co_3O_4	8.086	8.086	8.086	528.7

Table S3. XPS quantification data for all elements in Ir-Co_3O_4, Ru-Co_3O_4, Pd-Co_3O_4, Ir-NiO, and Ir-Fe_2O_3.

Compounds	Element	Atomic%
Ir-Co_3O_4	Ir	1.86
	Co	28.44
	O	69.70
Ru-Co_3O_4	Ru	1.41
	Co	21.24
	O	77.35
Pd-Co_3O_4	Pd	1.18
	Co	31.65
	O	67.17
Ir-NiO	Ir	0.75
	Ni	41.66
	O	57.58
Ir-Fe_2O_3	Ir	1.39
	Fe	26.06
	O	72.55

Table S4. Fitting parameters of EIS for Ir-Co_3O_4, IrO_2, and Co_3O_4 in 0.5 M H_2SO_4.

Samples	Rs (Ω)	Rct (Ω)	C_{dl} (F s^{n-1})	s (Ω $s^{-1/2}$)
Ir-Co_3O_4	5.1	16.6	0.0498	0.0498
IrO_2	4.0	220.0	0.1991	0.0498
Co_3O_4	5.1	5271.0	0.0996	4.5658

Table S5. Comparisons of the Tafel slopes and overpotentials at the current density of 10 mA cm^{-2} of reported Ir-based catalysts for OER in 0.5 M H_2SO_4.

Catalysts	Overpotential (mV)	Tafel slope (mV dec^{-1})	Ref.
$Rh_{22}Ir_{78}$ alloy NPs	292	101	[1]
Porous carbon-coated IrCo	270	71.8	[2]
IrO_2/CNT	293	67	[3]
TiN/IrO_2	313	65.5	[4]
Ir–SA@Fe@NCNT	250	58.2	[5]
IrO_2/GCNa	276	57	[6]
Ir_6Ag_9 nanotubes	297	60	[7]
Amorphous IrO_x NSs	250	47	[8]
Sr_2IrO_4	287	45	[9]
Li-IrO_x	290	39	[10]
Ir-Co_3O_4	268	38	This work

Table S6. Fitting parameters of EIS for Ir-Co_3O_4, IrO_2, and Co_3O_4 in 1.0 M KOH.

Samples	Rs (Ω)	Rct (Ω)	C_{dl} (F s^{n-1})	s (Ω $s^{-1/2}$)
Ir-Co_3O_4	4.3	14.6	0.0498	9.6399
IrO_2	3.9	102.2	0.0896	6.2364
Co_3O_4	4.0	445.3	0.0996	0.1216

References

[1] H. Guo, Z. Fang, H. Li, D. Fernandez, G. Henkelman, S. M. Humphrey, G. Yu, *ACS Nano* **2019**, 13, 13225.

[2] X. Sun, F. Liu, X. Chen, C. Li, J. Yu, M. Pan, *Electrochimica Acta* **2019**, 307, 206.

[3] J. Guan, D. Li, R. Si, S. Miao, F. Zhang, C. Li, *ACS Catalysis* **2017**, 7, 5983.

[4] H. Zhang, Z. Y. Yuan, B. Li, X. Jin, presented at *the 2019 Chinese Control And Decision Conference (CCDC)*, 3-5 June 2019, **2019**.

[5] F. Luo, H. Hu, X. Zhao, Z. Yang, Q. Zhang, J. Xu, T. Kaneko, Y. Yoshida, C. Zhu, W. Cai, *Nano Letters* **2020**, 20, 2120.

[6] J. Chen, P. Cui, G. Zhao, K. Rui, M. Lao, Y. Chen, X. Zheng, Y. Jiang, H. Pan, S. X. Dou, W. Sun, *Angewandte Chemie International Edition* **2019**, 58, 12540.

[7] M. Zhu, Q. Shao, Y. Qian, X. Huang, *Nano Energy* **2019**, 56, 330.

[8] B. Jiang, J. Kim, Y. Guo, K. C. W. Wu, S. M. Alshehri, T. Ahamad, N. Alhokbany, J. Henzie, Y. Yamachi, *Catalysis Science & Technology* **2019**, 9, 3697.

[9] A. L. Strickler, D. Higgins, T. F. Jaramillo, *ACS Applied Energy Materials* **2019**, 2, 5490.

[10] J. Gao, C.-Q. Xu, S.-F. Hung, W. Liu, W. Cai, Z. Zeng, C. Jia, H. M. Chen, H. Xiao, J. Li, Y. Huang, B. Liu, *Journal of the American Chemical Society* **2019**, 141, 3014.